Aust. J. Phys., 1986, 39, 15–23

Excitation of Swift Heavy Ions in Foil Targets. II* X-radiation from Br

H. J. Hay, L. F. Pender and P. B. Treacy

Department of Nuclear Physics, Research School of Physical Sciences, Australian National University, P.O. Box 4, Canberra, A.C.T. 2601.

Abstract

An experimental arrangement is described to detect delayed X-rays emitted following foil excitation of 130 MeV Br ions at distances to 190 mm downstream of a self-supporting carbon target. The intensities of L X-rays at a number of distances were measured. The observations are discussed in terms of the decay of high-n Rydberg ions. It is shown that, in addition to the expected yrast cascades, there are other little-understood cascades with high intensities.

1. Introduction

It is well known that swift ions after traversing foil targets emit radiations characteristic of states with a single electron of high principal quantum number n ($\gtrsim 10$) (Betz *et al.* 1980; Rothermel *et al.* 1980; Betz *et al.* 1982; Hay *et al.* 1983). The observed time decays of such states have been described approximately in terms of yrast chains, that is, states with maximum angular momentum $l = n-1$ de-exciting by electric dipole transitions in the steps $(n, l), (n-1, l-1)$... (Hasse *et al.* 1979). The lifetime of such high-n, high-l states is approximately $0\cdot 02 n^5/Z^4$ ns, where Z is the screened nuclear charge. The deduced initial (n, l) population of such states appears to deviate from the so-called statistical distribution with population proportional to n^{-5} per substate (n^{-3} per n value) which is predicted on the basis of various mechanisms (Betz 1980). Furthermore the charge and thickness dependence of excitation probabilities disagree with the predictions of simple models (Hay *et al.* 1983; Betz *et al.* 1983).

In studies of in-target X-ray production from 130 MeV Br ions in carbon, we have observed (Hay *et al.* 1982) that L X-rays are emitted characteristic of Rydberg states with n–n transitions 3–2 and 4–2 formed into two fairly well-defined distinct groups at energies $1\cdot 6$ and $2\cdot 2$ keV respectively. A spectrum from a 20 μg cm^{-2} carbon target is displayed in Fig. 1 (upper curve) with these two groups labelled Lα and Lβ respectively. This spectrum was obtained from a Si(Li) detector aimed directly at the target. It may be compared with the lower spectrum, obtained from ions 20 mm downstream of a similar target. In this ('beam–foil') spectrum, the two

* Part I, *Aust. J. Phys.*, 1983, 36, 7.

0004-9506/86/010015$02.00

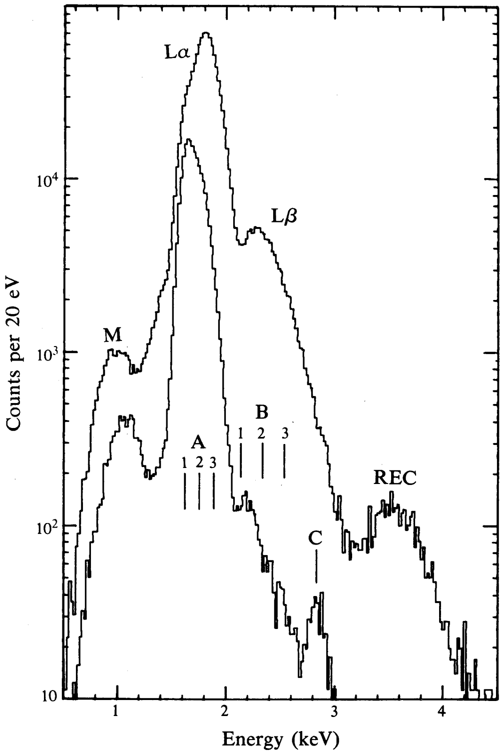

Fig. 1. X-ray spectra from bombardment of a 20 $\mu g\,cm^{-2}$ self-supporting target by 130 MeV ^{79}Br ions. Shown are the spectrum of 'in-target' X-rays obtained by direct detection at 45° to the beam axis (upper curve), and the beam–foil spectrum 20 mm downstream under the conditions depicted in Fig. 2 (lower curve). The labels M, Lα, etc. are defined in the text.

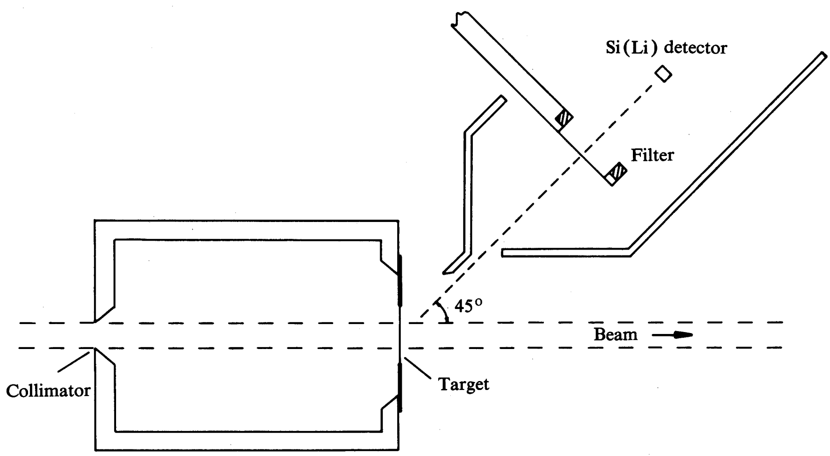

Fig. 2. Arrangement for detecting X-rays from foil-excited ions over a limited line-of-sight downstream of the target. The detector baffle plates, represented schematically in section, were devised to obtain a clear line-of-sight while minimizing detection of X-rays from the scattered beam.

main groups are still present after a time (≈ 1 ns) much greater than the expected in-target L-vacancy lifetime ($<0\cdot1$ ps). Comparison of the two spectra shows that the curve labelled 'REC' in the upper curve—corresponding to direct radiative electron capture of target electrons—has disappeared from the beam–foil spectrum, but a less intense and narrower group labelled C is now present at $2\cdot9$ keV. (In both spectra a low-energy X-ray labelled M appears near 1 keV. This is too strongly absorbed to permit quantitative analysis of its structure and intensity, and it will not be discussed further in this paper.)

Most previous beam–foil studies of delayed X-radiations have comprised observation of a final transition into the 1s ground state of 1- or 2-electron ions. The study of heavy ions stripped to the region of the L shell opens up the possibility of distinguishing between different decay routes, as in the spectra of Fig. 1. This can provide more information on the (n, l) dependence of the population of Rydberg states. It was the purpose of the present work to study the shapes of decay curves and absolute intensities of the different L X-rays shown in Fig. 1, in order to deduce more information on the populations of the classes of states which may feed them.

2. Experimental Method and Results

The target and detector arrangement used for recording beam–foil X-rays is illustrated in Fig. 2. A 130 MeV ^{79}Br beam from the A.N.U. 14UD accelerator, incident with charge state 10^{+}, is collimated to 4 mm diameter and passed through a 20 μg cm^{-2} self-supporting carbon target. The X-rays are detected in a 10 mm^2 Si(Li) detector of energy resolution 153 eV at $5\cdot9$ keV. The detector has a 8 μm Be window; additional filters can be inserted in front of it.

The length of beam path seen by the detector is limited by means of a baffle. Although the time resolution is inherently better when the beam is viewed at 90°, we chose to view at 45° so that the target could be traversed through the line-of-sight in order to establish both the time zero and the shape of the time resolution function of the experimental arrangement. (Only for a pure exponential decay is the observed decay constant independent of the resolution function.) The baffle plates needed to be as close to the beam as possible to improve the resolution, but they must not intercept the beam as ions would be re-excited.

From the geometry of the arrangement in Fig. 2, the profile of intensity against distance downstream was calculated to be trapezoidal with a width of $4\cdot6$ mm at half maximum. This may be compared with the results of a beam scan shown in Fig. 3, which was obtained by passing a self-supporting Cu target through the detector's line-of-sight and recording Cu K X-rays under bombardment of the target by 2 MeV protons. The observed width was $4\cdot7$ mm FWHM, and of a shape sufficiently sharp for reasonable analysis of data by a rectangular-profiled spatial resolution function.

Spectra were recorded at 23 positions between 8 and 190 mm from the target, by viewing both directly and through a 45 μm mylar filter. Data were normalized to the transmitted beam by charge collection in a Faraday cage.

The lower spectrum in Fig. 1 (recorded at 20 mm with no filter) represents a typical example of the data, where the observed peak shapes are not gaussian and are considerably wider than the detector resolution. Peak A in particular has distinguishable components, and it was decided to analyse it by dividing it into separate lines, each with a gaussian profile. However, it was not clear how many significant lines would be required for such an analysis. As a trial, each pair of spectra

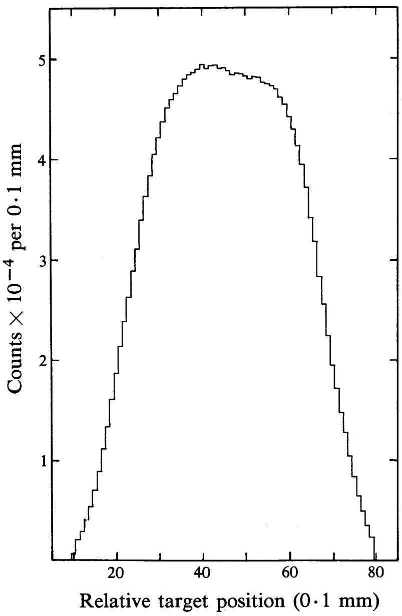

Fig. 3. Intensity distribution measured downstream by using the geometry of Fig. 2. This was obtained by stepping a thin Cu target in the beam direction through the detector line-of-sight and detecting Cu K X-rays produced in-target by an exciting 2 MeV proton beam.

(with and without absorbers) was fitted for each of the 23 different positions, by a nonlinear least-squares method (Hay 1969) with two lines. This proved unsatisfactory as the fitted line widths were unequal, that at the higher energy being about twice the lower, which was near the detector resolution, and these widths varied systematically with position. A similar analysis into three lines showed no such effects, apart from residual variations consistent with known electronics shifts due to temperature variations. Consequently peak A was analysed into a notional set of three equally spaced gaussian lines of widths which appeared equal to the detector resolution. Similarly the shape of peak B was accounted for by three equally spaced lines of equal width and wider than those of A; peak C was accounted for by a single line of the B-component width. These lines, of fixed energy and width, we designate A1-3, B1-3 and C. Fits to the data enabled the unabsorbed intensity to be extracted for each observed region downstream of the target. An example of such a fit is given in Fig. 4, in which the fitted no-absorber line spectrum has been multiplied by the mylar absorption coefficients and the result compared with the experimental mylar-absorbed spectrum; the fit is excellent. The energies of lines quoted below have been corrected for Doppler shifts.

In order to obtain yields of X-rays, normalized to the number of ions capable of emitting L X-rays, it is necessary to know the total number of X-rays emitted and the charge-state distribution of the beam. The total number of X-rays was calculated by assuming isotropic X-ray emission in the centre-of-mass, and allowing for the solid angle ($2\cdot 14\times 10^{-4}$ sr) of the detector. The charge-state distribution was obtained by a knowledge of the mean exit charge state (22·5), measured by Pender and Hay (1984), and by assuming that the 12% of emergent ions* of charge state 25^{+} (one vacancy and one excited electron) is the dominant source of delayed X-ray production.

* Charge-state fractions of emergent ions were measured in a subsidiary experiment. The sum of all fractions with more than one L vacancy was 3%.

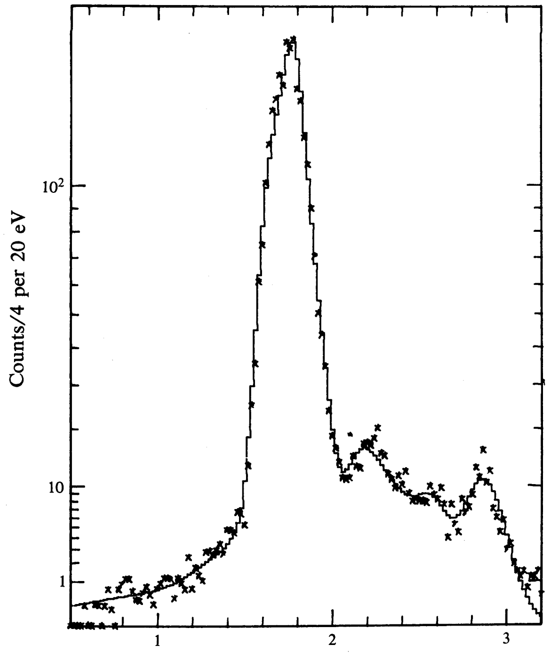

Fig. 4. Data (crosses) from an X-ray spectrum transmitted through a 45 μm mylar filter at 20 mm downstream. The full curve is a prediction based on the analysis of unfiltered spectra as shown in Fig. 1, and calculated using mylar absorption coefficients at the finite number (seven) of X-ray lines assumed present.

3. Discussion of Results

(a) Normalized Decay Rates

In order to interpret the data in terms of initial-state populations in quantum numbers (n, l) it was necessary to deduce, from the spectra fitted as in Fig. 4, plots of the normalized decay curves of the various L X-rays, and interpret these in terms of likely modes of decay. Before discussing such decay curves it is necessary to identify the probable physically distinct lines of those (seven) notionally defined in Section 2. Peak A, from its change of shape with decay, contains at least two lines; the relatively weak line A3 is not significantly different from a 'tail' to A2. Conversely, peak B certainly comprises many lines, and no clear physical identity can be claimed for each of the notional three. For these reasons, we designate henceforth four lines: A1, A2+A3, ΣB and C. These groupings are consistent with the fact that the decay rates of the lines within groups are the same within statistical errors (see Table 1 in Section 3*b*).

The decay curves obtained are illustrated in Fig. 5. These curves have not been adjusted, as they should in principle, due to the fact that at each downstream distance a profile of the form of Fig. 3 was sampled. Trial convolutions showed that such adjustment is not significant within the accuracy of the data, except for the very steeply falling A1 group at times below 0·8 ns. The implied change of slope there will not be discussed further.

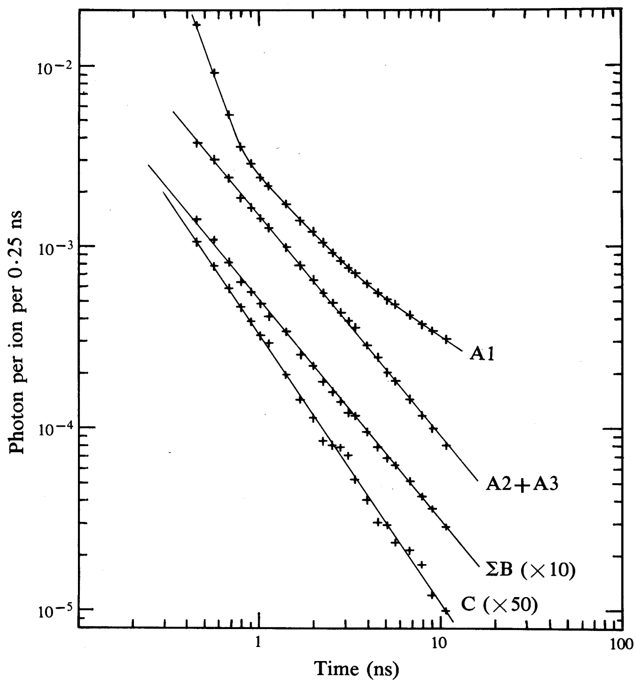

Fig. 5. Decay curves of X-ray lines. Fitted straight lines have the decay indices listed in Table 1. Components with indistinguishable indices have been combined in the graph. The curve for the A1 group is an 'eyeball' fit. The data were normalized absolutely to the measured beam as described in Section 3*a*.

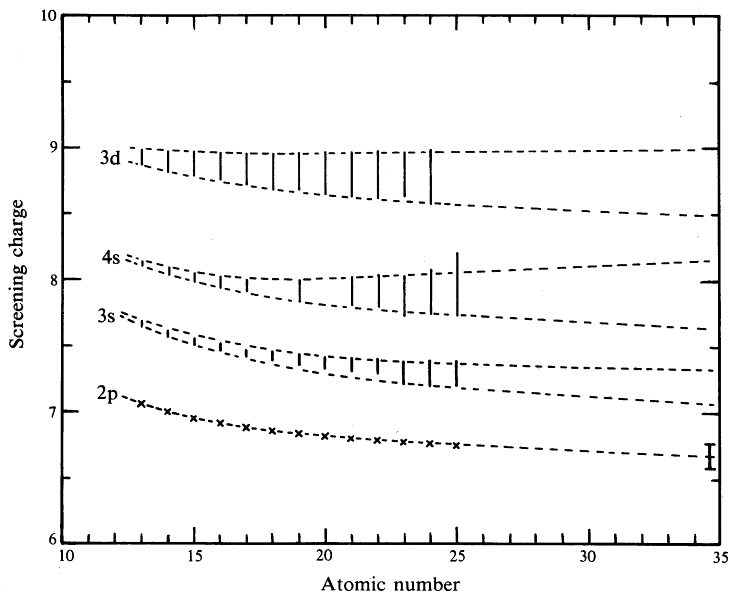

Fig. 6. Representation of effective screening charge for neon-like (10 electron) ionic spectra. The data, with errors representing spreads of tabulated values, were taken as described in Section 3*b* from the compilations of Bashkin and Stoner (1975, 1976, 1981).

(b) Identification of Transition

From the observed grouping of decay curves, as illustrated in Fig. 5, one might anticipate that the four lines represented by A1, A2+A3, ΣB and C ought to be identifiable with well-defined subshells of the L, M and higher shells. Such an identification was indeed found possible with the aid of Grotrian diagrams (Bashkin and Stoner 1975, 1976, 1981) by using information on the term energies of ions of other species which correspond to the 10-electron neon-like ion under study. The method is illustrated in Fig. 6 which shows a plot of the screening charge (q) that is required empirically to bring the known term energy in each species (Z), with the core configuration $1s^2 2s^2 2p^5$, to a hydrogenic form, namely

$$E_T = 13\cdot6(Z-q)^2/n^2 \text{ eV}.$$

Such a representation provided essentially a convenient parameter (q) with which to extrapolate E_T with an estimate of its uncertainty, out to the value $Z = 35$ for Br. Fig. 6 shows that this may be done with some confidence.

Table 1. Assignment of L X-rays by energy and substate transition

Lines are indicated in the notation defined in Section 2 and the groupings of Fig. 5. Substate assignments are in hydrogenic notation

Peak	Fitted energy (eV)^A	Gaussian FWHM (eV)	Intensity^B	Time decay power	Centroid (eV)	Predicted energy (eV)	Substate transition
				Analysis peak			
A1	1560	130	230				
A2	1687	130	120				
A3	1814	130	20				
B1	2054	230	3·0				
B2	2246	230	1·0				
B3	2438	230	0·5				
C	2725	230	0·5				
				Grouped peak			
A1				Note^C	1560	1560±10	[3s–2p]
A2+A3				1·214±0·006	1705	1680±20	[3d–2p]
ΣB				1·210±0·009	2140	2150±10	[4f–2p]
C				1·46±0·03	2725	2723±10	$n \gtrsim 10$, $l = 0$ or 2

^A A common width and separation were assumed for all A and for all B components, as explained in the text.
^B Intensity 20 mm downstream; units are 10^{-5} photons per ion per 0·25 ns, i.e. the scale of the ordinate in Fig. 5.
^C The A1 power decreases steadily from 2·8 to 0·7 over the range 8–190 mm.

The results are summarized in Table 1, which proposes unique identification of the four X-ray 'lines'. The fact, mentioned in Section 2, that all of these but A1 are of fitted widths greater than that of the detector resolution, is attributable partly to subshell splittings and also to the different term energies of other ions in the beam which have more than one L vacancy. Examination of the Grotrian diagrams for 9-electron ions (Br charge state 26^+) indicated that the line energies would be raised by approximately 100 eV. Such lines could contribute to the broadening of the B and C groups observed. However, since the 26^+ fraction is less than a quarter of the 25^+

fraction of ions in the beam and since the decays are of order $(26/25)^4$ times faster (Bethe and Salpeter 1957), they will occur at times some 15% earlier and will have little effect on the shapes of the curves in Fig. 5.

(c) Qualitative Interpretation of Decay Curves

From the assignments of Table 1, it is to be expected that the groups A2+A3 and ΣB correspond to the bottom transition of the yrast chain and an E2 branch, respectively; their intensity ratio of 30 : 1 is in accordance with such a branching (Bethe and Salpeter 1957). Then, in terms of the well-defined power laws of Fig. 5, namely $t^{-1\cdot 21}$, one may deduce from the theory of Hasse *et al.* (1979) that the yrast chain could follow an *initial* population $n^{-\beta}$ with $\beta = 2\cdot 26$. A statistical population would be represented by $\beta = 4$, although the apparent value would always be reduced by up to one unit as a result of 'collapsing' via direct transitions, from non-yrast states onto the yrast line. The degree to which the apparent value of 2·26 may be affected by such collapsing will be discussed elsewhere.

A natural interpretation of the relatively weak C group is direct transitions from high-n, low-l states, i.e. ($n \gtrsim 10$, $l = 0$ or 2) to (2, p). This is based on the reasonable assumption that the ion's L vacancy has achieved its lowest-energy state prior to the earliest time of observation (0·44 ns) which is already longer than the lifetime of $l = 0$–2 states with n less than 30. For example, as shown by Bethe and Salpeter (1957), lifetimes for $l = 0$ states have values $2n^3/Z^4$ ns, where Z is defined in Section 1. The observed power-law decay of $t^{-1\cdot 46}$ is consistent with an *initial* population with $\beta = 2\cdot 38$.

The most intense group (A1) does not follow a power-law decay and clearly does not correspond to direct or yrast transitions with a unique β value. If the explanation above of the observed C group is correct, one must expect, in a similar way, that there will be some high-n to (3, 0) transitions contributing to A1. Based on a sum of two populations (two β values) a fit to the shape of the decay may be obtained, but it corresponds to an initial population of the order 10^{10} electrons per ion—see the enormously increasing slope of its decay curve towards low decay times in Fig. 5. Arbitrary cutoffs in the n populations could improve this at the expense of the fit. The data fit better a single power-law decay $t^{-1\cdot 15}$ plus an exponential decay with lifetime 110 ps and an effectively *constant* background decay rate of 0·06% per ns. Such a decay scheme is, in fact, qualitatively consistent with the possibility that certain M-shell states populated by direct or yrast decays must be 'blocked' from decaying directly to the single L vacancy, and a slow two-stage decay to the ground state occurs. A very interesting possibility for the small constant decay is that of post-foil feeding of the 3s population by convoy electrons (Sellin *et al.* 1982; Betz *et al.* 1983). Both possibilities must be regarded as speculative. One must conclude, therefore, that the major ($\approx$80%) intensity of the post-foil radiation of ions observed in our experiment is little understood at the present time.

References

Bashkin, S., and Stoner, J. O. (1975, 1976, 1981). 'Atomic Energy Levels and Grotrian Diagrams', Vols 1–3 (North-Holland: New York).

Bethe, H. A., and Salpeter, E. E. (1957). 'Quantum Mechanics of One and Two Electron Atoms' (Springer: Berlin).

Betz, H.-D. (1980). *In* 'Atomic Physics: Accelerators' (Ed. P. Richard) (Academic: New York).

Betz, H.-D., Röschenthaler, D., and Rothermel, J. (1983). *Phys. Rev. Lett.* **50**, 34.
Betz, H.-D., Rothermel, J., and Bell, F. (1980). *Nucl. Instrum. Methods* **170**, 243.
Betz, H.-D., Rothermel, J., Röschenthaler, D., Bell, F., Schuch, R., and Nolte, G. (1982). *Phys. Lett.* A **91**, 12.
Hasse, R. W., Betz, H.-D., and Bell, F. (1979). *J. Phys.* B **12**, L711.
Hay, H. J. (1969). *In* 'Least Squares Methods in Data Analysis' (Eds R. S. Andersson and M. R. Osborne), p. 70 (A.N.U.: Canberra).
Hay, H. J., Newton, C. S., and Treacy, P. B. (1983). *Aust. J. Phys.* **36**, 7.
Hay, H. J., Pender, L. F., and Treacy, P. B. (1982). *J. Phys.* B **15**, L331.
Pender, L. F., and Hay, H. J. (1984). *Phys. Rev. Lett.* **50**, 1174.
Rothermel, J., Betz, H.-D., and Bell, F. (1980). *Nucl. Instrum. Methods* **194**, 341.
Sellin, I. A., Breinig, M., Brandt, W., and Laubert, R. (1982). *Nucl. Instrum. Methods* **194**, 395.

Manuscript received 8 July, accepted 24 October 1985